Histone Deacetylase Inhibitors Up-Regulate the Expression of Tight Junction Proteins

Mauro Bordin,[1,2] Fabio D'Atri,[1] Laurent Guillemot,[1] and Sandra Citi[1,2]

[1]Department of Molecular Biology, University of Geneva, Geneva, Switzerland and [2]Department of Biology, University of Padova, Padova, Italy

Abstract

Histone deacetylase (HDAC) inhibitors promote cell maturation, differentiation, and apoptosis through changes in gene expression. Differentiated epithelial cells are characterized by apical tight junctions (TJ), which play a role in cell-cell adhesion, polarity, and the permeability barrier function of epithelia. The relationship between cellular differentiation and expression of TJ-associated proteins is not known. Here, we investigated whether HDAC inhibitors affect the expression of TJ proteins in cultured cells by immunoblotting, immunofluorescence, and quantitative real-time, reverse transcription-PCR. We find that the HDAC inhibitor sodium butyrate significantly up-regulates the protein levels of cingulin, ZO-1, and ZO-2 in Rat-1 fibroblasts, cingulin in COS-7 cells, and cingulin and occludin in HeLa cells. Levels of mRNA for cingulin, ZO-1, and ZO-2 are also increased in sodium butyrate–treated Rat-1 fibroblasts. Up-regulation of cingulin is reversible and dose dependent and requires *de novo* protein synthesis and protein kinase activity, because it is inhibited by cycloheximide and by the protein kinase inhibitor H-7. Up-regulation of TJ proteins by sodium butyrate is linked to the ability of sodium butyrate to inhibit HDAC activity, because suberoylanilide hydroxamic acid, a HDAC inhibitor of a different structural class, also up-regulates cingulin, ZO-1, and ZO-2 expression in Rat-1 fibroblasts. These results indicate that cellular differentiation correlates with kinase-dependent up-regulation of the expression of specific TJ proteins.
(Mol Cancer Res 2004;2(12):692–701)

Introduction

The short-chain fatty acid sodium butyrate is produced naturally in the colonic lumen by microbial fermentation of dietary fiber and is believed to physiologically regulate epithelial cell maturation in the intestinal tract by modulating the pathways of proliferation, differentiation, and apoptosis (1). *In vitro*, sodium butyrate and related compounds inhibit cell proliferation and induce cellular differentiation and apoptosis in many cell types, including colon cancer cells (2, 3), breast cancer cells (4), prostate cancer cells (5), leukemia cells (6), and myogenic precursors and tumors (7, 8). The mechanism of action of sodium butyrate involves inhibition of histone deacetylase (HDAC) activity (9), which is followed by changes in chromatin structure and de-repression of a fraction of cellular genes (10). The ability of sodium butyrate to inhibit cell proliferation and promote differentiation and apoptosis has prompted studies on the use of butyrate-related compounds as therapeutic antitumor agents in human neoplasias (reviewed in ref. 11).

Differentiation can be defined as the gain of structural and functional features of mature cells through the expression of specific gene products that regulate cell shape, function, adhesion, and communication. Differentiated epithelial cells show apico-basal polarity and contain apical tight junctions (TJ). TJ seal neighboring cells within epithelial sheets, thereby creating a semipermeable barrier, which separates different body and organ compartments. In addition, TJ separate the apical from basolateral domain of the plasma membrane and thus contribute to the maintenance of the polarized epithelial phenotype (12). TJ comprise a large number of protein components, including membrane proteins such as occludin (reviewed in ref. 13), and cytoplasmic proteins such as ZO-1, ZO-2, and cingulin (reviewed in ref. 14). Some of the cytoplasmic components of TJ are evolutionarily conserved and play important roles in the development of apico-basal polarity in vertebrates and invertebrates (15). However, the role of most TJ proteins in the maturation of the polarized phenotype and in epithelial differentiation is unknown. This question is complicated by the observation that certain TJ-associated proteins are expressed not only in TJ-bearing cells but also in nonepithelial cells and tissues. For example, ZO-1 can be found associated with cadherin-based adherens-type junctions in fibroblasts and other nonepithelial cells and tissues (16). Thus, the relationship between expression of TJ proteins and differentiation of epithelial and other cell types remains an open question.

In this study, we addressed this question by asking whether differentiation induced by HDAC inhibitors is associated with changes in the expression of specific TJ proteins in cultured cells. In addition, we used drugs that interfere with different signaling pathways to explore the molecular mechanisms of action of HDAC inhibitors. For our studies, we used cultured "fibroblastic" cell lines, which typically express no or low levels of TJ-specific proteins, and epithelial-derived cell lines, including the cervical carcinoma line HeLa, which express some

Received 7/7/04; revised 9/24/04; accepted 10/27/04.
Grant support: Swiss Cancer League, Swiss National Science Foundation, Ministry for Italian University and Research, ERASMUS Program (M. Bordin), and Roche Research Foundation fellowship (L. Guillemot).
The costs of publication of this article were defrayed in part by the payment of page charges. This article must therefore be hereby marked advertisement in accordance with 18 U.S.C. Section 1734 solely to indicate this fact.
Requests for reprints: Sandra Citi, Department of Molecular Biology, University of Geneva, 30 Quai Ernest Ansermet, 1211 Geneva 4, Switzerland. Phone: 41-22-3796182; Fax: 41-22-3796868. E-mail: Sandra.Citi@molbio.unige.ch

but not all of the TJ proteins that we examined. Our results show that in several of these cell lines HDAC inhibitors lead to up-regulation of specific TJ proteins through mechanisms that require protein kinase activity and *de novo* protein synthesis. These results suggest that modulation of the expression of specific TJ proteins plays a role in cellular differentiation.

Results

Sodium Butyrate Dramatically Up-Regulates Cingulin Expression in Rat-1 Fibroblasts

Rat-1 fibroblasts are an established fibroblastoid 3T3-like cell line obtained by SV40 transformation of a permanent line derived from Fisher rat embryos (17). Rat-1 fibroblasts do not form TJ and are not known to express TJ membrane proteins, although they express ZO-1, which is localized at adherens-type junctions (18).

Confluent Rat-1 monolayers were treated with 10 mmol/L sodium butyrate for 16 hours, and the cell morphology was examined by phase-contrast microscopy. Control cultures contained a homogeneous layer of cells with an elongated shape (Fig. 1A and A′). Cultures treated with sodium butyrate were overlaid by clumps of round cells, consistent with the known ability of sodium butyrate to induce apoptosis (*arrowheads* in Fig. 1B). The monolayer contained occasional gaps, and the cells appeared more spread out (Fig. 1B′).

Confocal immunofluorescence microscopy was used to study the expression and localization of TJ-associated proteins (Fig. 1C-H). We chose cingulin, ZO-1, ZO-2, and occludin as marker proteins, because previous studies indicate that cingulin and occludin are expressed in an epithelium-specific manner, whereas ZO-1 and ZO-2 have also been detected in non-epithelial cells (19-23). In epithelial cells, these proteins are associated in a multiprotein complex (24). In optical sections of untreated fibroblasts, no junctional labeling was detected with anti-cingulin antiserum (Fig. 1C, E, and G), although faint staining was occasionally detected on isolated cells by conventional microscopy (data not shown), indicating that cingulin is expressed in Rat-1 fibroblasts at very low levels. In contrast, ZO-1 staining was clearly distributed along the junctional regions of all cells (Fig. 1C′), in a pattern of contiguous segments of different length, which were oriented at different angles but often perpendicular with respect to the cell border (*arrowheads* in Fig. 1C′). Control cells stained for ZO-2 showed cytoplasmic and nuclear staining and undetectable junctional labeling (Fig. 1E′). The nuclear localization of ZO-2 has been reported previously (25). No labeling for occludin was detected in untreated Rat-1 fibroblasts (Fig. 1G′).

Upon sodium butyrate treatment, cingulin staining became clearly detectable along cell-cell junctions (Fig. 1D and D") and was precisely colocalized with ZO-1 (Fig. 1D′ and D) in a pattern of contiguous segments that were typically oriented parallel to the cell border. Similarly, on sodium butyrate treatment, there was an increase in ZO-2 labeling, which was detectable mostly in the cytoplasm or nucleus and weakly at junctions, where it was colocalized with cingulin (*arrowhead* in Fig. 1F, F′, and F′′). In contrast, sodium butyrate treatment did not result in detectable expression of occludin as determined by immunofluorescence (Fig. 1H′ and H").

To analyze the expression of cingulin, ZO-1, ZO-2, and occludin at the protein level, lysates from untreated and sodium butyrate–treated cultures were analyzed by SDS-PAGE and immunoblotting (Fig. 1I). In lysates of untreated Rat-1 fibroblasts, the cingulin signal was either undetectable or extremely faint, confirming that cingulin is expressed in Rat-1 fibroblasts at barely detectable levels. In contrast, lysates of sodium butyrate–treated cultures contained a clearly labeled $M_r \sim 140$-kDa polypeptide, which was recognized by anti-cingulin antibodies and comigrated with cingulin from Madin-Darby canine kidney (MDCK) epithelial cells (Fig. 1I). ZO-1 and ZO-2 were clearly detected in lysates from untreated Rat-1 fibroblasts, and their levels were increased in sodium butyrate–treated cell lysates (Fig. 1I). Densitometric analysis of immunoblots showed that ZO-1 levels were increased $\sim 2.5 \pm 0.27$-fold ($n = 3$) and ZO-2 levels were increased $\sim 2.5 \pm 0.05$-fold ($n = 3$) when cultures were treated with HDAC inhibitors. In contrast, no occludin was detected in control or sodium butyrate–treated Rat-1 lysates by immunoblotting (Fig. 1I). Taken together, these observations show that, in Rat-1 fibroblasts, sodium butyrate up-regulates, to different extents, the protein levels of cingulin, ZO-1, and ZO-2. The lack of detection of occludin, a major constituent of the membrane domain of TJ, shows that not all TJ proteins are up-regulated by sodium butyrate in these cells and suggests that functional TJ may not be formed. Confirming this notion, measurement of the transepithelial resistance showed that no significant paracellular permeability barrier was measured across monolayers of Rat-1 fibroblasts regardless of sodium butyrate treatment (data not shown).

To study in more detail the induction of TJ protein expression by sodium butyrate, we analyzed the dose dependence, time course, and reversibility of sodium butyrate activity (Fig. 2). We focused our analysis on cingulin expression, because the previous experiments indicated that cingulin was the protein that showed the most dramatic up-regulation in response to sodium butyrate treatment. Analysis of lysates from cells incubated with different concentrations of sodium butyrate for 16 hours showed that significant cingulin protein was detected starting at 1 mmol/L sodium butyrate and the maximal effect was seen between 2 and 10 mmol/L (Fig. 2A). When cells were incubated with 10 mmol/L sodium butyrate, protein expression was detected by immunoblotting at 5 hours after the beginning of treatment and maximal up-regulation was detected between 16 and 24 hours (Fig. 2B). To determine whether the effect of sodium butyrate is reversible, cultures were treated with 10 mmol/L sodium butyrate for 16 hours; then, the sodium butyrate–containing medium was removed and replaced with normal medium, and cells were lysed at different times after sodium butyrate removal. Immunoblotting showed that cingulin progressively decreased 24 and 48 hours after sodium butyrate removal, and no cingulin was detected 72 hours after the removal of sodium butyrate (Fig. 2C). Thus, the up-regulation of cingulin expression by sodium butyrate in Rat-1 cells is dose and time dependent and reversible.

Cingulin Up-Regulation Is Blocked by the Protein Kinase Inhibitor H-7 and by Protein Synthesis Inhibitors

To investigate the molecular mechanisms and the signaling pathways, which control up-regulation of cingulin expression by

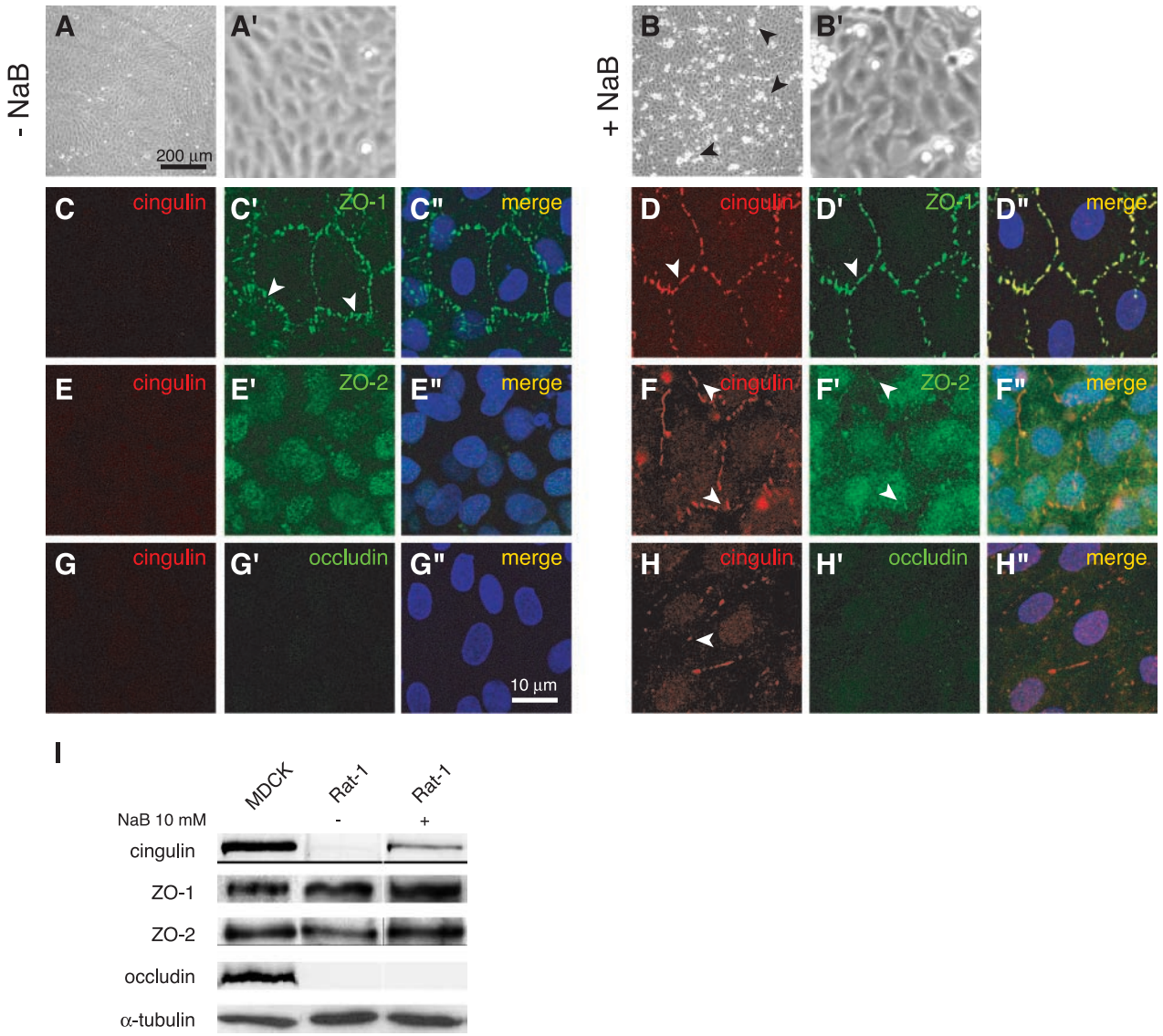

FIGURE 1. Sodium butyrate (*NaB*) up-regulates cingulin, ZO-1, and ZO-2 in Rat-1 fibroblasts. **A-H.** Rat-1 fibroblasts were incubated either without (**A**, **C**, **E**, and **G**) or with (**B**, **D**, **F**, and **H**) sodium butyrate for 16 hours and observed by phase-contrast microscopy (**A** and **B**) or by confocal fluorescence microscopy after fixation and immunolabeling with antibodies against cingulin [polyclonal antibody (**C** and **D**) and monoclonal antibody (**E-H**)], ZO-1 [monoclonal antibody (**C′** and **D′**)], ZO-2 [polyclonal antibody (**E′** and **F′**)], and occludin [polyclonal antibody (**G′** and **H′**)]. Merge images (**C-H**) also show 4′,6-diamidino-2-phenylindole-stained nuclei. **B.** *Arrowheads,* clumps of Rat-1 cells (probably apoptotic) above the monolayer. **C′.** *Arrowheads,* labeling for ZO-1 in untreated cells in a pattern of segments oriented toward the cell center. **D**, **D′**, **F**, and **F′.** *Arrowheads,* junctional staining of cingulin colocalized with ZO-1 and ZO-2, respectively, in a pattern of segments oriented parallel to the cell-cell border. Polyclonal anti-cingulin antibodies also label centrosomes (not detected in these confocal optical sections) possibly due to a nonspecific cross-reaction. Bar, 200 μm (**A** and **B**) and 10 μm (**C-H**). **I.** Immunoblot analysis: total lysates of epithelial MDCK cells (MDCK-positive control) and Rat-1 fibroblasts (Rat-1) were analyzed by SDS-PAGE followed by immunoblotting with the antibodies against cingulin (M_r 140 kDa), ZO-1 (M_r ~225 kDa), ZO-2 (M_r ~160 kDa), occludin (M_r ~60 kDa), and α-tubulin (M_r ~50 kDa; control for protein loading). −, no treatment; +, treatment with sodium butyrate (10 mmol/L, 16 hours). Note that sodium butyrate treatment induces increased labeling of the cingulin, ZO-1, and ZO-2 polypeptides.

sodium butyrate, Rat-1 cells were treated with sodium butyrate in the presence of agents that are known to interfere with a variety of intracellular enzyme activities, signaling pathways, or the organization of the actin and microtubule cytoskeletons.

The protein kinase inhibitor H-7 selectively prevents the formation of TJ, but not adherens-type junctions, in cultured epithelial cells (26). We thus hypothesized that H-7 might affect cingulin up-regulation in response to sodium butyrate treatment. Immunoblot analysis showed that when 5 μmol/L H-7 was added to the culture medium in the presence of sodium butyrate, cingulin expression was still detectable (Fig. 3A). However, no cingulin was detected in the presence of 100 or 10 μmol/L H-7 (Fig. 3A). Thus, the serine/threonine protein kinase inhibitor H-7 blocks up-regulation of cingulin by HDAC inhibitors.

We next tested whether valproic acid, another short-chain fatty acid inhibitor of HDAC (27), is also effective in

inducing cingulin up-regulation. Immunoblot analysis (Fig. 3A) and immunofluorescence (data not shown) showed that the effect of valproic acid on cingulin expression is indistinguishable from that of sodium butyrate and is equally inhibited by H-7 (Fig. 3A). Because both sodium butyrate and valproic acid have several actions that may not be a consequence of inhibition of HDAC (28), we investigated the effect of suberoylanilide hydroxamic acid (SAHA), a more potent and specific HDAC inhibitor, on the expression of cingulin and ZO-2 in Rat-1 fibroblasts. Immunoblot analysis showed that SAHA induces up-regulation of cingulin and ZO-2 (Fig. 3B) as well as ZO-1 (data not shown), confirming the notion that up-regulation of TJ proteins is the consequence of inhibition of HDAC. Conversely, no cingulin up-regulation was detected when cells were treated with 5-azacytidine, a DNA methylation inhibitor that can promote epithelial differentiation of mesenchymal cells (ref. 29; data not shown).

We then asked whether cingulin up-regulation is a consequence of *de novo* protein synthesis rather than being due to an increase in protein stability. Treatment of Rat-1 fibroblasts with anisomycin at concentrations that inhibit translation (10 μg/mL) blocked sodium butyrate–induced cingulin expression (Fig. 3C). The same suppression of cingulin expression was obtained with the protein synthesis inhibitor cycloheximide (Fig. 3C). Thus, cingulin up-regulation by sodium butyrate requires *de novo* protein synthesis.

Because H-7 can affect the organization of the actomyosin cytoskeleton (30) and cingulin binds to actin filaments (31), we tested whether inhibition of sodium butyrate–induced cingulin up-regulation could be influenced by microfilament- or microtubule-active drugs. Treatment of cells with sodium butyrate in the presence of cytochalasin D (data not shown) and nocodazole (Fig. 3C) were still associated with increased cingulin expression, indicating that disruption of the cytoskeleton does not affect sodium butyrate–induced cingulin up-regulation.

Because H-7 inhibits not only protein kinase C (PKC) but also other kinases, we used additional signaling inhibitors and activators to identify pathways involved in sodium butyrate–induced cingulin up-regulation. Immunoblot analysis showed that cingulin up-regulation by sodium butyrate was not inhibited by the ROCK kinase inhibitor Y27632 (Fig. 3D), the cell-permeable PKCζ/λ pseudosubstrate (PKCζ inhibitor; Fig. 3D), the protein kinase A inhibitor H-89, and the tyrosine kinase inhibitor genistein (data not shown). Treatment of cells with the PKC activator phorbol 12-myristate 13-acetate neither induced cingulin expression in control cells nor prevented sodium butyrate–induced cingulin expression (Fig. 3D), suggesting that typical PKC is not involved.

Activation or inhibition of mitogen-activated protein kinase pathways has been implicated in the development and maintenance of differentiated or transformed phenotypes in several cultured cell types (6, 32). In addition, mitogen-activated protein kinase/extracellular signal-regulated kinase kinase activity is required for claudin-mediated formation of TJ (33). We therefore tested whether treatment of Rat-1 fibroblasts with drugs that inhibit or activate mitogen-activated protein kinase pathways affects sodium butyrate–induced cingulin expression. No effect on sodium butyrate–mediated induction of cingulin was observed using the mitogen-activated protein kinase/extracellular signal-regulated kinase kinase1/2 inhibitor U0126 (Fig. 3D), the p38 inhibitor SB203580, or the Jun NH_2-terminal kinase and p38 agonist

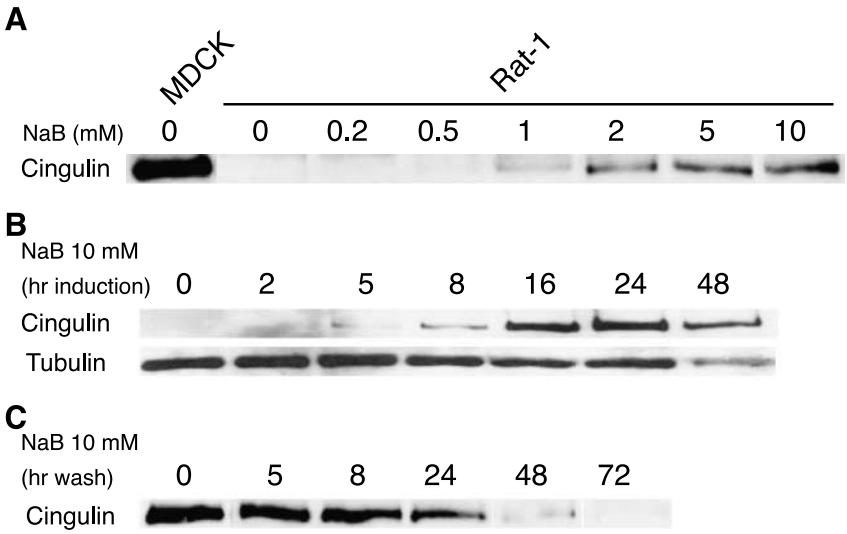

FIGURE 2. Cingulin up-regulation by sodium butyrate is dose and time dependent and reversible. **A.** Rat-1 fibroblasts were incubated for 16 hours in the presence of the indicated concentrations of sodium butyrate, and total lysates were analyzed by immunoblotting with anti-cingulin antiserum. *MDCK lane,* migration of the M_r 140-kDa cingulin polypeptide. **B.** Rat-1 fibroblasts were treated with 10 mmol/L sodium butyrate for the indicated lengths of time (hours), and total lysates were analyzed by immunoblotting with anti-cingulin antiserum and anti-tubulin antibodies. Note that maximal cingulin staining is observed between 16 and 24 hours, whereas at 48 hours the intensity of cingulin and tubulin labeling decreases probably as a consequence of apoptosis-induced loss of cells from the monolayer (**C**). Cells were treated with sodium butyrate for 16 hours, rinsed with normal medium, and incubated (wash) with normal medium for the indicated lengths of time before preparation of lysates. *Left,* migration of the M_r 140-kDa cingulin and M_r ~50-kDa tubulin polypeptides.

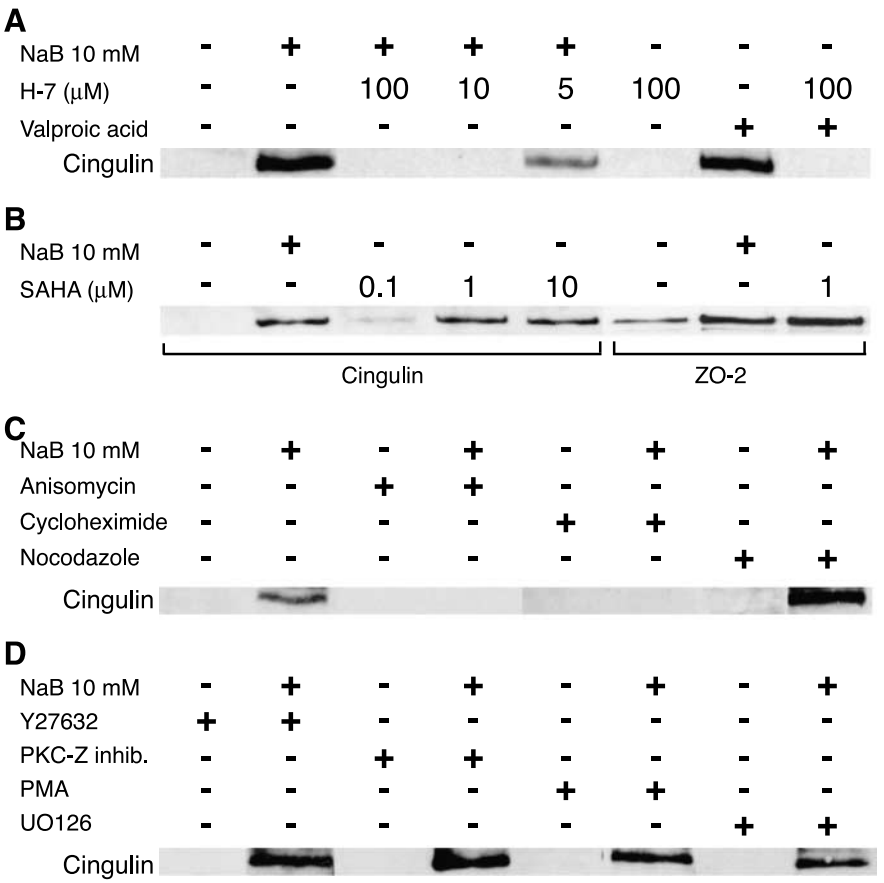

FIGURE 3. H-7 and protein synthesis inhibitors prevent cingulin up-regulation by HDAC inhibitors. **A-D.** Immunoblot analysis was done with anti-cingulin antiserum (**A**, **C**, **D**, and *bracketed lanes* in **B**) and with anti-ZO-2 antibodies (*bracketed lanes* in **B**) on total lysates of Rat-1 fibroblasts prepared from cells incubated with different drugs. *Left,* drugs; –, absence of the drug; *+,* presence of the drug in the culture medium (16 hours). Sodium butyrate was used at a concentration of 10 mmol/L and the concentrations of H-7 (**A**) and SAHA (**B**) are indicated above each lane (μmol/L). Concentrations for other drugs are indicated in Materials and Methods.

anisomycin (at the subinhibitory concentration of 50 ng/mL; data not shown). Finally, studies on cultured hepatoma cells indicated that sodium butyrate may act through phosphatases (34). However, the phosphatase inhibitors okadaic acid or H_2O_2 did not prevent sodium butyrate–mediated cingulin expression (data not shown).

Sodium Butyrate and H-7 Display Antagonistic Effects on mRNA Levels for Cingulin, ZO-1, and ZO-2

To explore the effect of H-7 on the transcript levels of TJ proteins, which are up-regulated by sodium butyrate (cingulin, ZO-1, and ZO-2), quantitative real-time, reverse transcription-PCR was done on RNA isolated from Rat-1 cells (Table 1). Difference in threshold cycle values (ΔC_t) was obtained using the 18S RNA as the internal control, and fold changes in mRNA levels were calculated by measuring the variation in ΔC_t value ($\Delta\Delta C_t$; see Materials and Methods). Sodium butyrate induced an increase in mRNA levels by 2.8-fold for cingulin, 2.5-fold for ZO-1, and 1.9-fold for ZO-2. H-7 not only reversed the sodium butyrate–induced increase in mRNA levels but also, by itself, dramatically reduced transcript levels for cingulin, ZO-1, and ZO-2 (Table 1). Thus, the sodium butyrate–induced increase in cingulin, ZO-1, and ZO-2 proteins, as detected by immunoblot, correlated with an increase in their respective mRNA levels, and H-7 influenced both protein and mRNA levels.

Sodium Butyrate Up-Regulates Cingulin and Occludin in Other Cell Types

To establish whether up-regulation of TJ protein expression by sodium butyrate is restricted to Rat-1 fibroblasts or occurs in other cultured cell types, we examined by immunoblotting the effect of sodium butyrate on the expression of cingulin, ZO-1, ZO-2, and occludin in Chinese hamster ovary (CHO), COS-7, HeLa, and 3T3 cell lines. Cingulin expression was also analyzed by immunofluorescence.

No specific junctional cingulin labeling was detected by immunofluorescence in CHO cells regardless of treatment with sodium butyrate (Fig. 4A and A′). Rarely, cells showed diffuse, nonspecific cytoplasmic labeling that was not affected by sodium butyrate treatment. In lysates of CHO cells, the $M_r \sim 140$-kDa cingulin polypeptide was not labeled, whereas a cross-reacting $M_r \sim 150$-kDa polypeptide was detected (*asterisk* in Fig. 4E). This $M_r \sim 150$ kDa may correspond to paracingulin (Genbank accession no. AAT37906), a protein that shows partial homology to cingulin. In contrast, ZO-1 and ZO-2 polypeptides were clearly detected by immunoblotting in CHO lysates, and their levels were not affected by sodium butyrate treatment (Fig. 4E). Occludin was not detected in CHO lysates (Fig. 4E).

In COS-7 cells, the anti-cingulin antiserum stained the regions of cell-cell contact in a linear pattern (*arrow* in Fig. 4B), and the intensity of staining increased on sodium butyrate treatment (Fig. 4B′). A $M_r \sim 140$-kDa polypeptide, which comigrated with

mammalian cingulin, was detected in COS-7 lysates by immunoblotting analysis, and its intensity increased in lysates from sodium butyrate–treated cells (Fig. 4E). In contrast, ZO-1 and ZO-2 were not detected in COS-7 lysates, possibly due to lack of cross-reactivity of antibodies (Fig. 4E). However, occludin was clearly detectable, and its levels were not affected by sodium butyrate treatment.

Junctional labeling by anti-cingulin antibodies was detected by immunofluorescence in the regions of cell-cell contact in HeLa cells in a discontinuous pattern (Fig. 4C). Upon sodium butyrate treatment, the intensity of the immunofluorescent labeling increased significantly (Fig. 4C′). Analysis of HeLa cell lysates by immunoblotting showed that the $M_r \sim 140$-kDa cingulin polypeptide was detected in control cells, and its levels increased on sodium butyrate treatment (Fig. 4E). In addition, a cross-reacting $M_r \sim 150$-kDa polypeptide was labeled by anti-cingulin antibodies in HeLa cell lysates, but its levels were not affected by sodium butyrate treatment (Fig. 4E). ZO-1 and ZO-2 polypeptides were detected by immunoblotting in both control and sodium butyrate–treated HeLa cell cultures, and their levels were not affected by sodium butyrate treatment (Fig. 4E). In contrast, sodium butyrate treatment induced the expression of occludin in HeLa cells as determined by immunoblotting (Fig. 4E). Occludin was also detectable by immunofluorescence only in sodium butyrate–treated cells (Fig. 4C′) and was colocalized with cingulin (Fig. 4C). Despite the expression of occludin, no significant TJ barrier function was detected by measurement of transepithelial resistance in HeLa monolayers (data not shown). This may be due to the fact that TJ proteins were not distributed in a continuous ring along the cell-cell border (Fig. 3C′), thus preventing the establishment of a functional seal.

In 3T3 cells, the anti-cingulin antiserum labeled the regions of cell-cell contact in a faint, discontinuous, granular pattern (Fig. 4D), and the intensity of staining was slightly increased on sodium butyrate treatment (Fig. 4D′). A $M_r \sim 140$-kDa polypeptide was barely detectable by immunoblotting in lysates of control 3T3 cells and more intensely stained in sodium butyrate–treated fibroblasts (Fig. 4E). ZO-1 was also barely detectable in lysates of 3T3 cells, whereas ZO-2 and occludin were not detected (Fig. 4E).

Taken together, these observations indicate that cellular differentiation induced by HDAC inhibitors correlates with cingulin up-regulation not only in Rat-1 fibroblasts but also in COS-7, HeLa, and, to a lesser extent, 3T3 cells. In contrast, occludin up-regulation was only detected in HeLa cells, and ZO-1 and ZO-2 up-regulation was only detected in Rat-1 fibroblasts.

Discussion

The results presented here provide biochemical, morphologic, and molecular evidence that the expression of specific TJ proteins is up-regulated during cellular differentiation induced by HDAC inhibitors in several cultured cell types and that protein kinase activity is required for this up-regulation.

The identity of factors and signaling mechanisms, which promote epithelial differentiation, is a question of considerable biological significance. During development and epithelial morphogenesis, cells acquire apico-basal polarity and assemble junctions that mediate cell-cell adhesion, tissue sorting, and separation of tissue compartments. With regard to disease states, many cancer cells fail to achieve complete cell differentiation and show a phenotype of maturation arrest together with unregulated proliferation. Significantly, loss or down-regulation of cell-cell junctions in malignant cancer cells can lead to increased cell migration and metastasis (35), and recent studies suggest that TJ proteins are also implicated in cancer. For example, a significant correlation has been observed between decreased tumor differentiation or histologic grade and ZO-1 (36), ZO-2 (37), and claudin-7 expression (38) in breast carcinomas. In addition, down-regulation of occludin has been shown to play an important role in the loss of TJ induced by Ras/Raf-driven epithelial transformation (39). Finally, cingulin expression was detected in poorly differentiated colon adenocarcinomas but not in nonepithelial cancers (40), suggesting that cingulin is an epithelium-specific marker. All these observations indicate a correlation between different levels of cellular differentiation and the expression of specific TJ proteins. However, nothing was known until this study about the effect of differentiating agents such as HDAC inhibitors on the expression of TJ proteins.

It was shown previously that the differentiating agent sodium butyrate affects the morphology and cytoskeletal organization of cultured cells (reviewed in ref. 41) and the expression of several cytoskeletal proteins, including intermediate filament proteins (42), actin (43), and nonmuscle myosin (44). In addition, sodium butyrate has been shown to induce stabilization of desmosomes in MDCK cells (45) and increased expression and junctional recruitment of cadherin and catenin in colon cancer cells (46).

TABLE 1. Sodium Butyrate and H-7 Show Antagonistic Effects on mRNA Levels of TJ Proteins in Rat-1 Fibroblasts

	ΔC_t				Fold Change		
	Control	+ Sodium Butyrate	+ H-7	+ Sodium Butyrate + H-7	Sodium Butyrate versus Control	Sodium Butyrate + H-7 versus Sodium Butyrate	H-7 versus Control
Cingulin	15.9 ± 0.1	14.4 ± 0.1	17.9 ± 0.3	17.1 ± 0.3	↑ 2.8	↓ 6.5	↓ 4.0
ZO-1	13.3 ± 0.2	12.0 ± 0.1	13.8 ± 0.2	15.8 ± 0.2	↑ 2.5	↓ 13.9	↓ 1.4
ZO-2	15.2 ± 0.1	14.3 ± 0.2	21.4 ± 0.2	19.2 ± 0.2	↑ 1.9	↓ 30.1	↓ 73.5

NOTE: ΔC_t values represent the difference between the C_t value of the indicated gene and the C_t value of the 18S RNA gene used as an internal control. Relative increases/decreases (fold change) in mRNA levels are indicated by arrows and were calculated according to the formula $2^{-(\Delta\Delta C_t)}$. Note that sodium butyrate up-regulates mRNA levels, whereas H-7 down-regulates mRNA levels and reverses the effect of sodium butyrate.

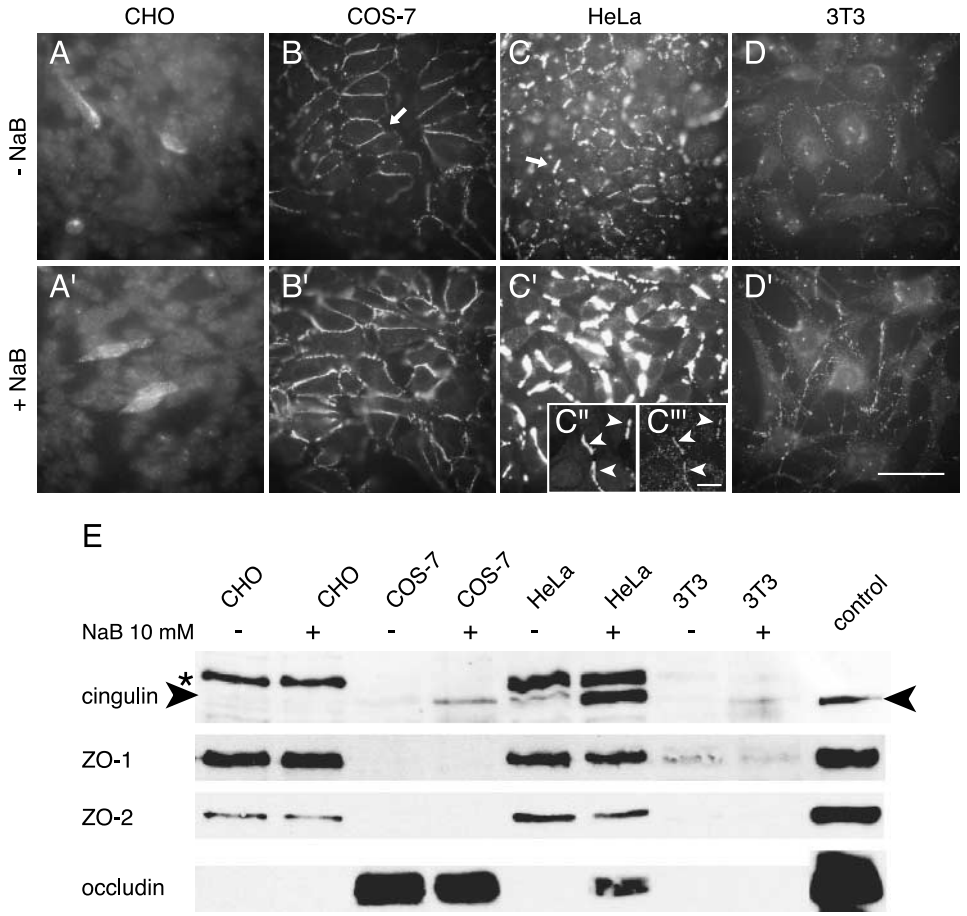

FIGURE 4. Effect of sodium butyrate on the expression of TJ proteins in CHO, COS-7, HeLa, and 3T3 cell lines. **A**, **D**, **A′**, and **D′**. Immunofluorescence analysis shows the localization of cingulin in control cells (**A**-**D**) and in cells treated with sodium butyrate (**A′**-**D′**). **B** and **C.** *Arrows,* cingulin junctional labeling in COS-7 and HeLa cells, respectively. **C′.** *Insets,* colocalization (*arrowheads*) of cingulin (**C′′**) and occludin (**C′′′**) in sodium butyrate–treated HeLa cells. Bar, 20 μm. **E.** Immunoblot analysis of total lysates from CHO, COS-7, HeLa, and 3T3 cells using antibodies against cingulin, ZO-1, ZO-2, and occludin. –, untreated cells; +, cells treated with sodium butyrate. A lysate of MDCK cells was used as a positive control. *Arrowhead,* migration of the M_r ~ 140-kDa cingulin polypeptide; *asterisk,* cross-reacting M_r ~ 150-kDa polypeptide, which is not up-regulated following sodium butyrate treatment.

Now, we show that HDAC inhibitors belonging to two different structural classes (sodium butyrate, valproic acid, and SAHA) up-regulate the expression of TJ proteins in different cultured cell lines. The response to sodium butyrate treatment is cell type dependent because up-regulation of TJ proteins was not observed in all cell lines. Cingulin up-regulation was strongest and was detected in most of the cell lines we examined, suggesting that cingulin may be a more sensitive marker of cellular differentiation than ZO-1 or ZO-2, at least in the cell types we examined. The notion that cingulin expression is linked to epithelial differentiation is supported by the observation that cingulin is expressed in several simple and stratified polarized epithelial tissues but shows no or very low levels of expression in nonepithelial tissues such as muscle, lens, and neural tissue (19, 40). In addition, the human cingulin gene is mapped to the same chromosomal locus (*1q21*; ref. 47) as the epidermal differentiation complex, which consists of multiple families of clustered genes that are generally expressed in epithelial cells and undergo coordinated regulation during keratinocyte differentiation (48). Finally, targeted mutation of the cingulin gene in mouse embryonic stem cells results in altered levels of expression of genes involved in endodermal differentiation (GATA-4, GATA-6, HNF4α, etc.) only when embryonic stem cells are stimulated to differentiate by growth in suspension (49). Indeed, differentiation of embryonic stem cells into embryoid bodies was found to be correlated with increased mRNA levels for most TJ protein genes (49).

How could expression of specific TJ proteins affect cellular differentiation? First, increased levels of TJ proteins could negatively regulate cell migration by affecting cell-cell adhesion either by acting directly as cell-cell adhesion molecules (e.g., occludin) or by strengthening the cytoskeletal scaffold underlying the plasma membrane. Second, formation of the TJ would provide epithelial sheets with a barrier function and thus regulate the diffusion of signaling molecules across tissue compartments. Last but not least, up-regulation of TJ proteins could indirectly affect gene expression. It has long been known that cytoplasmic levels of the junctional protein β-catenin are linked to regulation of transcriptional activity through the interaction of β-catenin with the factor LEF-TCF1 (50). Recent evidence also points to TJ proteins as potential regulators of transcription. The transcription factors ZONAB, huASH1, c-*fos*, and c-*jun* have been localized at TJ (51–53). ZONAB, a ZO-1-binding protein, regulates cell density and proliferation in epithelial monolayers, possibly through interaction with cell division kinase 4 (54). One current hypothesis is that, when the monolayer is confluent, TJ proteins bind to and sequester transcription factors such as ZONAB at TJ, thus preventing them from acting in the nucleus and stimulating cell proliferation (55). Thus, pharmacologic or physiologic up-regulation of TJ proteins may not only be a consequence of altered gene expression during differentiation but may also in turn contribute to regulating the activity of transcription factors and controlling cell proliferation and apoptosis.

In our study, we also sought to explore the contribution of different signaling pathways to the up-regulation of cingulin expression by sodium butyrate. Among several signaling activators and inhibitors that we tested, only protein synthesis inhibitors and the protein kinase inhibitor H-7 could block sodium butyrate–induced cingulin up-regulation. In contrast, drugs that interfere with the integrity of the actin and microtubule cytoskeleton and the activity of a variety of other signaling molecules did not prevent cingulin up-regulation by sodium butyrate. Interestingly, H-7 induced a decrease in mRNA levels for TJ proteins even in the absence of sodium butyrate, suggesting that a constitutive kinase activity is required to maintain mRNA levels of TJ protein genes. We showed previously that H-7 selectively prevents the assembly of TJ in cultured renal cells and suppresses cingulin up-regulation during TJ assembly (26, 56). Because atypical PKCζ/λ is involved in the establishment of epithelial TJ (57), one candidate target kinase for H-7 is atypical PKC. However, because the PKCζ inhibitor did not prevent cingulin up-regulation, a more likely candidate is the PKCε isoform, which is required for expression of $p21^{WAF1/Cip1}$ in cells treated with HDAC inhibitors (58, 59).

In summary, this study provides the first evidence that TJ proteins are up-regulated in a kinase-dependent manner during differentiation of cultured cells induced by HDAC inhibitors. Up-regulation of cingulin and other TJ proteins may represent an early step in the differentiation of cells toward an epithelial phenotype before the recruitment of TJ membrane proteins and final maturation of TJ. In addition, up-regulation of TJ proteins during differentiation may contribute to the regulation of the activity of transcription factors through their sequestration at junctions. Further studies on the role of specific TJ proteins in this and other experimental model systems should help to clarify the molecular mechanisms underlying physiologic and pathologic events in epithelial morphogenesis.

Materials and Methods

Cell Culture and Treatment with Sodium Butyrate

Rat embryonic cells (Rat-1), CHO cells, monkey kidney cells (COS-7), human epithelial cervical tumor cells (HeLa), mouse fibroblast cells (3T3), and dog kidney cells (MDCK cells; used for preparation of control lysates) were cultured in a humidified incubator at 37°C and 6% CO_2 in DMEM (high glucose, Invitrogen, Carlsbad, CA) supplemented with 10% FCS and nonessential amino acids. Cultures were plated on glass coverslips for immunofluorescence, on 60-mm diameter dishes for preparation of cell lysates, and on Transwell filters (Costar, Cambridge, MA) for measurement of transepithelial resistance using a Millicel-ERS apparatus.

A stock solution (1 mol/L) of sodium butyrate (Sigma, St. Louis, MO, B-5887, reconstituted in culture medium and stored in aliquots at −20°C) was added to the culture medium of confluent cultures to obtain the desired final concentration (typically 10 mmol/L). Alternatively, cells were treated with either valproic acid (Sigma P-4543, 2 mmol/L final concentration) or SAHA (Alexis, Lausen, Switzerland, 270-288-M001, 0.1-10 μmol/L final concentration). Cells were incubated with the HDAC inhibitors for different lengths of time (typically 16 hours) and either fixed for immunofluorescence or lysed. Measurement of transepithelial resistance was carried out on monolayers seeded at confluent density and cultured on Transwell filters for 48 hours before sodium butyrate treatment.

Treatment of Rat-1 Fibroblasts with Signaling Inhibitors and Activators

The following drugs were used: anisomycin (Sigma A-9789, final concentration 0.05-10 μg/mL), 5′-azacytidine (Sigma A-2385, 5 μg/mL), cytochalasin D (Sigma C-8273, 10 μmol/L), cycloheximide (Sigma C-7698, 10 μg/mL), H_2O_2 (Sigma H-1009, 50 μmol/L), H-7 (Sigma I-7016, 5-100 μmol/L), H-89 (Sigma B-1427, 100 μmol/L), PKCζ inhibitor (Biosource, Camarillo, CA, 77-748, 20 μmol/L), nocodazole (Sigma M-1404, 0.2 μg/mL), okadaic acid (Sigma O-7760, 100 nmol/L), phorbol 12-myristate 13-acetate (Sigma P-8139, 100 nmol/L), SB203580 (Calbiochem, La Jolla, CA, 559389, 10 μmol/L), U0126 (Promega, Madison, WI, V1121, 50 μmol/L), and Y27632 (Tocris, Ellisville, MO, 1254, 10 μmol/L). The drugs were added to the cells ~10 minutes before addition of sodium butyrate by diluting stock solutions into the culture medium. The drugs remained in the medium throughout the sodium butyrate treatment. Control cultures were treated with solvent alone.

Immunofluorescence

Immunofluorescent staining of cells on glass coverslips was done by rinsing cells in PBS [136 mmol/L NaCl, 2.6 mmol/L KCl, 10 mmol/L Na_2HPO_4, 1.7 mmol/L KH_2PO_4 (pH 7.4)], fixing for 5 minutes in methanol (at −20°C), washing with PBS, and incubating with primary antibody (1 hour, room temperature) followed by washes in PBS, incubation with secondary antibody (45 minutes, room temperature), washing, and mounting. The following antibodies were used: rabbit anti-cingulin (Zymed, South San Francisco, CA, 36-4401, 1:500), mouse anti-cingulin (Zymed 37-4300, 1:50), rabbit anti-ZO-1 (Zymed 61-7300, 1:100), rabbit anti-ZO-2 (Zymed 71-1400, 1:200), and rabbit anti-occludin (Zymed 33-1500, 1:100). Secondary antibodies (The Jackson Laboratory, Bar Harbor, ME) were labeled with FITC, TRITC, or Cy5 and used at a dilution of 1:200. Specimens were observed with a Zeiss Axiovert S100TV microscope using a 63× planApo (1.3 NA) objective for immunofluorescence, and a 10× Plan-Neofluar objective for phase contrast. Images were acquired with a Hamamatsu C4742-95 CCD camera controlled by Openlab software. For confocal microscopy, we used a Zeiss LSM-510 Meta system, and 1-μm-thick optical sections were imaged.

Preparation of Cell Lysates and Immunoblotting

To prepare total cell lysates for immunoblotting, cultures on 60-mm dishes were rinsed twice with cold PBS, incubated in 0.25 mL radioimmunoprecipitation assay buffer [150 mmol/L NaCl, 40 mmol/L Tris-HCl (pH 7.6), 2 mmol/L EDTA, 10% glycerol, 1% Triton X-100, 0.5% sodium deoxycholate, 0.2% SDS, 5 μg/mL antipain-leupeptin-pepstatin cocktail, 1 mmol/L phenylmethylsulfonyl fluoride] at 4°C for 10 minutes, scraped from the dish, and sonicated (Branson Digital Sonifier, 5 seconds at 33% amplitude). Protein loadings were normalized

by staining immunoblots with antibodies against α-tubulin. Gels were transferred electrophoretically onto nitrocellulose (0.1 A, 12 hours, 4°C) and probed with the indicated antibodies (at the dilutions recommended by the manufacturer) followed by alkaline phosphatase–labeled (Promega) or horseradish peroxidase–labeled (Amersham, Arlington Heights, IL) secondary antibodies. The chromogenic substrate nitroblue tetrazolium/5-bromo-4-chloro-3-indolyl phosphate (Sigma B-1911) or the chemiluminescent reagent SuperSignal WestPico (Pierce, Rockford, IL, 34080) were used to reveal the antibody reaction.

Quantitative Real-time, Reverse Transcription-PCR

Total RNA was prepared from Rat-1 fibroblasts using the RNeasy mini kit (Qiagen, Valencia, CA). Sodium butyrate–treated cultures were incubated with 10 mmol/L sodium butyrate for 16 hours before RNA preparation. cDNA synthesis was achieved with 1 to 2 μg of total RNA using the iScript cDNA synthesis kit (Bio-Rad). SYBR green-based real-time PCR was used to measure relative gene expression in each sample using 96-well plates. Each master mix (25 μL) contained a single gene-specific primer set (forward and reverse, 2.5 μmol/L), 20 ng of cDNA, 10 nmol/L fluorescein calibration dye, and 2× SYBR Green PCR Mastermix (Applied Biosystems, Foster City, CA). Each experimental sample was assayed using three replicates for each primer, including the 18S RNA specific primer, which was used as an internal standard. Negative controls lacking the cDNA template were run with every assay to assess specificity. Gene-specific primer sets were designed using Primer-Express software (Applied Biosystems) and were as follows: 18S RNA forward 5′-ACATCCAAGGAAGGCAGCAG-3′, 18S RNA reverse 5′-TTTTCGTCACTACCTCCCCG-3′, cingulin forward 5′-AGTCAGACCGTGTGGCTTTTG-3′, cingulin reverse 5′-CTGAAGGGCCACATTGCTCT-3′, ZO-1 forward 5′-GAGCTACGCTTGCCACACTGT-3′, ZO-1 reverse 5′-TCGGATCTCCAGGAAGACACTT-3′, ZO-2 forward 5′-TCAGAGCCGGTGCAGCA-3′, and ZO-2 reverse 5′-TCATCTGAGCGCGTGGC-3′. The real-time fluorescence signal was analyzed using the iCycler iQ software version 3.0 (Bio-Rad). The cycling conditions were as follows: 1 cycle at 95°C for 10 minutes followed by 40 cycles of PCR amplification, each consisting of 95°C for 15 seconds and 60°C for 45 seconds. To identify specific PCR products, melting curve analysis was done by heating the reaction mixture from 60°C to 95°C at the rate of 0.5°C per 10 seconds. A threshold cycle (C_t) was determined for each sample using the exponential growth phase and the baseline signal from fluorescence versus cycle number plots. PCR assays that showed nonspecific products at the end point were excluded from further data analysis. ΔC_t values were obtained by subtracting the C_t value of the housekeeping gene 18S RNA from the C_t value for each indicated gene. Each ΔC_t value represents the mean ± SD of three independent experiments. $\Delta\Delta C_t$ was calculated as the difference in ΔC_t between different samples. Positive $\Delta\Delta C_t$ values indicate a higher number of PCR cycles and therefore a lower amount of mRNA. Conversely, negative $\Delta\Delta C_t$ values indicate higher amounts of mRNA. The fold change was calculated by $2^{-(\Delta\Delta Ct)}$.

References

1. Augenlicht LH, Mariadason JM, Wilson A, et al. Short chain fatty acids and colon cancer. J Nutr 2002;132:3804–8S.

2. Barnard JA, Warwick G. Butyrate rapidly induces growth inhibition and differentiation in HT-29 cells. Cell Growth Differ 1993;4:495–501.

3. Litvak DA, Evers BM, Hwang KO, Hellmich MR, Ko TC, Townsend CM Jr. Butyrate-induced differentiation of Caco-2 cells is associated with apoptosis and early induction of $p21^{Waf1/Cip1}$ and $p27^{Kip1}$. Surgery 1998;124:161–9; discussion 169–70.

4. Graham KA, Buick RN. Sodium butyrate induces differentiation in breast cancer cell lines expressing the estrogen receptor. J Cell Physiol 1988;136:63–71.

5. Maier S, Reich E, Martin R, et al. Tributyrin induces differentiation, growth arrest and apoptosis in androgen-sensitive and androgen-resistant human prostate cancer cell lines. Int J Cancer 2000;88:245–51.

6. Witt O, Sand K, Pekrun A. Butyrate-induced erythroid differentiation of human K562 leukemia cells involves inhibition of ERK and activation of p38 MAP kinase pathways. Blood 2000;95:2391–6.

7. Fiszman MY, Montarras D, Wright W, Gros F. Expression of myogenic differentiation and myotube formation by chick embryo myoblasts in the presence of sodium butyrate. Exp Cell Res 1980;126:31–7.

8. Dexter DL, Konieczny SF, Lawrence JB, Shaffer M, Mitchell P, Coleman JR. Induction by butyrate of differentiated properties in cloned murine rhabdomyosarcoma cells. Differentiation 1981;18:115–22.

9. Riggs MG, Whittaker RG, Neumann JR, Ingram VM. *n*-Butyrate causes histone modification in HeLa and Friend erythroleukaemia cells. Nature 1977;268:462–4.

10. Van Lint C, Emiliani S, Verdin E. The expression of a small fraction of cellular genes is changed in response to histone hyperacetylation. Gene Expr 1996;5:245–53.

11. Spira AI, Carducci MA. Differentiation therapy. Curr Opin Pharmacol 2003;3:338–43.

12. Schneeberger EE, Lynch RD. The tight junction: a multifunctional complex. Am J Physiol Cell Physiol 2004;286:C1213–28.

13. Tsukita S, Furuse M, Itoh M. Multifunctional strands in tight junctions. Nat Rev Mol Cell Biol 2001;2:285–93.

14. D'Atri F, Citi S. Molecular complexity of vertebrate tight junctions. Mol Membr Biol 2002;19:103–12.

15. Knust E, Bossinger O. Composition and formation of intercellular junctions in epithelial cells. Science 2002;298:1955–9.

16. Howarth AG, Hughes MR, Stevenson BR. Detection of the tight junction-associated protein ZO-1 in astrocytes and other nonepithelial cell types. Am J Physiol 1992;262:C461–9.

17. Topp WC. Normal rat cell lines deficient in nuclear thymidine kinase. Virology 1981;113:408–11.

18. D'Atri F, Nadalutti F, Citi S. Evidence for a functional interaction between cingulin and ZO-1 in cultured cells. J Biol Chem 2002;277:27757–64.

19. Citi S, Sabanay H, Kendrick-Jones J, Geiger B. Cingulin: characterization and localization. J Cell Sci 1989;93:107–22.

20. Itoh M, Nagafuchi A, Yonemura S, Yasuda-Kitani T, Tsukita S, Tsukita S. The 220kD protein colocalizing with cadherins in non-epithelial cells is identical to ZO-1, a tight junction-associated protein in epithelial cells: cDNA cloning and immunoelectron microscopy. J Cell Biol 1993;121:491–502.

21. Furuse M, Hirase T, Itoh M, et al. Occludin: a novel integral membrane protein localizing at tight junctions. J Cell Biol 1993;123:1777–88.

22. Aaku-Saraste E, Hellwig A, Huttner WB. Loss of occludin and functional tight junctions, but not ZO-1, during neural tube closure-remodeling of the neuroepithelium prior to neurogenesis. Dev Biol 1996;180:664–79.

23. Inoko A, Itoh M, Tamura A, Matsuda M, Furuse M, Tsukita S. Expression and distribution of ZO-3, a tight junction MAGUK protein, in mouse tissues. Genes Cells 2003;8:837–45.

24. Cordenonsi M, D'Atri F, Hammar E, et al. Cingulin contains globular and coiled-coil domains and interacts with ZO-1, ZO-2, ZO-3, and myosin. J Cell Biol 1999;147:1569–82.

25. Islas S, Vega J, Ponce L, Gonzalez-Mariscal L. Nuclear localization of the tight junction protein ZO-2 in epithelial cells. Exp Cell Res 2002;274:138–48.

26. Denisenko N, Burighel P, Citi S. Different effects of protein kinase inhibitors on the localization of junctional proteins at cell-cell contact sites. J Cell Sci 1994;107:969–81.

27. Gottlicher M, Minucci S, Zhu P, et al. Valproic acid defines a novel class of HDAC inhibitors inducing differentiation of transformed cells. EMBO J 2001;20:6969–78.

28. Marks PA, Miller T, Richon VM. Histone deacetylases. Curr Opin Pharmacol 2003;3:344–51.

29. Darmon M, Nicolas JF, Lamblin D. 5-Azacytidine is able to induce the conversion of teratocarcinoma-derived mesenchymal cells into epithelia cells. EMBO J 1984;3:961–7.

30. Volberg T, Geiger B, Citi S, Bershadsky AD. The effect of protein kinase inhibitor H-7 on the contractility, integrity and membrane anchorage of the microfilament system. Cell Motil Cytoskeleton 1994;29:321–38.

31. D'Atri F, Citi S. Cingulin interacts with F-actin *in vitro*. FEBS Lett 2001;507:21–4.

32. Ding Q, Wang Q, Evers BM. Alterations of MAPK activities associated with intestinal cell differentiation. Biochem Biophys Res Commun 2001;284:282–8.

33. Kinugasa T, Sakaguchi T, Gu X, Reinecker HC. Claudins regulate the intestinal barrier in response to immune mediators. Gastroenterology 2000;118:1001–11.

34. Cuisset L, Tichonicky L, Jaffray P, Delpech M. The effects of sodium butyrate on transcription are mediated through activation of a protein phosphatase. J Biol Chem 1997;272:24148–53.

35. Behrens J. Cadherins and catenins: role in signal transduction and tumor progression. Cancer Metastasis Rev 1999;18:15–30.

36. Hoover KB, Liao SY, Bryant PJ. Loss of the tight junction MAGUK ZO-1 in breast cancer: relationship to glandular differentiation and loss of heterozygosity. Am J Pathol 1998;153:1767–73.

37. Chlenski A, Ketels KV, Korovaitseva GI, Talamonti MS, Oyasu R, Scarpelli DG. Organization and expression of the human zo-2 gene (tjp-2) in normal and neoplastic tissues. Biochim Biophys Acta 2000;1493:319–24.

38. Kominsky SL, Argani P, Korz D, et al. Loss of the tight junction protein claudin-7 correlates with histological grade in both ductal carcinoma *in situ* and invasive ductal carcinoma of the breast. Oncogene 2003;22:2021–33.

39. Li D, Mrsny RJ. Oncogenic Raf-1 disrupts epithelial tight junctions via downregulation of occludin. J Cell Biol 2000;148:791–800.

40. Citi S, Amorosi A, Franconi F, Giotti A, Zampi G. Cingulin, a specific protein component of tight junctions, is expressed in normal and neoplastic human epithelial tissues. Am J Pathol 1991;138:781–9.

41. Kruh J. Effects of sodium butyrate, a new pharmacological agent, on cells in culture. Mol Cell Biochem 1982;42:65–82.

42. Borenfreund E, Schmid E, Bendich A, Franke WW. Constitutive aggregates of intermediate-sized filaments of the vimentin and cytokeratin type in cultured hepatoma cells and their dispersal by butyrate. Exp Cell Res 1980;127:215–35.

43. Ryan MP, Borenfreund E, Higgins PJ. Butyrate-induced cytoarchitectural reorganization of Mallory body-containing rat hepatic tumor cells. J Natl Cancer Inst 1987;79:555–67.

44. Buxton DB, Golomb E, Adelstein RS. Induction of nonmuscle myosin heavy chain II-C by butyrate in RAW 264.7 mouse macrophages. J Biol Chem 2003;278:15449–55.

45. Bogner P, Skehan P, Kenney S, Sainz E, Akeson MA, Friedman SJ. Stabilization of intercellular contacts in MDCK cells during Ca^{2+} deprivation. Selective effects of monocarboxylic acids on desmosomes. J Cell Sci 1992;103:463–73.

46. Barshishat M, Polak-Charcon S, Schwartz B. Butyrate regulates E-cadherin transcription, isoform expression and intracellular position in colon cancer cells. Br J Cancer 2000;82:195–203.

47. Citi S, D'Atri F, Parry DAD. Human and *Xenopus* cingulin share a modular organization of the coiled-coil rod domain: predictions for intra- and intermolecular assembly. J Struct Biol 2000;131:135–45.

48. Engelkamp D, Schafer BW, Mattei MG, Erne P, Heizmann CW. Six S100 genes are clustered on human chromosome 1q21: identification of two genes coding for the two previously unreported calcium-binding proteins S100D and S100E. Proc Natl Acad Sci U S A 1993;90:6547–51.

49. Guillemot L, Hammar E, Kaister C, et al. Disruption of the cingulin gene does not prevent tight junction formation but alters gene expression. J Cell Sci. 2004;117:5245–56.

50. Behrens J, von Kries JP, Kuhl M, et al. Functional interaction of β-catenin with the transcription factor LEF-1. Nature 1996;382:638–42.

51. Balda MS, Matter K. The tight junction protein ZO-1 and an interacting transcription factor regulate ErbB-2 expression. EMBO J 2000;19:2024–33.

52. Nakamura T, Blechman J, Tada S, et al. huASH1 protein, a putative transcription factor encoded by a human homologue of the *Drosophila* ash1 gene, localizes to both nuclei and cell-cell tight junctions. Proc Natl Acad Sci U S A 2000;97:7284–9.

53. Betanzos A, Huerta M, Lopez-Bayghen E, Azuara E, Amerena J, Gonzalez-Mariscal L. The tight junction protein ZO-2 associates with Jun, Fos and C/EBP transcription factors in epithelial cells. Exp Cell Res 2004;292:51–66.

54. Balda MS, Garrett MD, Matter K. The ZO-1-associated Y-box factor ZONAB regulates epithelial cell proliferation and cell density. J Cell Biol 2003;160:423–32.

55. Balda MS, Matter K. Epithelial cell adhesion and the regulation of gene expression. Trends Cell Biol 2003;13:310–8.

56. Citi S, Denisenko N. Phosphorylation of the tight junction protein cingulin and the effect of protein kinase inhibitors and activators in MDCK epithelial cells. J Cell Sci 1995;108:2917–26.

57. Suzuki A, Yamanaka T, Hirose T, et al. Atypical protein kinase C is involved in the evolutionarily conserved par protein complex and plays a critical role in establishing epithelia-specific junctional structures. J Cell Biol 2001;152:1183–96.

58. Kim YK, Han JW, Woo YN, et al. Expression of p21(WAF1/Cip1) through Sp1 sites by histone deacetylase inhibitor apicidin requires PI 3-kinase-PKC epsilon signaling pathway. Oncogene 2003;22:6023–31.

59. Kobayashi H, Tan EM, Fleming SE. Acetylation of histones associated with the $p21^{WAF1/Cip1}$ gene by butyrate is not sufficient for $p21^{WAF1/Cip1}$ gene transcription in human colorectal adenocarcinoma cells. Int J Cancer 2004;109:207–13.

Molecular Cancer Research

Histone Deacetylase Inhibitors Up-Regulate the Expression of Tight Junction Proteins [1]1Swiss Cancer League, Swiss National Science Foundation, Ministry for Italian University and Research, ERASMUS Program (M. Bordin), and Roche Research Foundation fellowship (L. Guillemot).

Mauro Bordin, Fabio D'Atri, Laurent Guillemot, et al.

Mol Cancer Res 2004;2:692-701.